How to cite: *Angew. Chem. Int. Ed.* **2023**, *62*, e202315156
doi.org/10.1002/anie.202315156

NIR Emitters

High-Performance Near-Infrared Chlorinated Rylenecarboximide Fluorophores via Consecutive C–N and C–C Bond Formation

Ze-Hua Wu, Artem Skabeev, Yulian Zagranyarski, Ruomeng Duan, Jun-O Jin, Minseok Kwak, Thomas Basché, Klaus Müllen,* and Chen Li**

Abstract: A new class of near-infrared (NIR) fluorophores, **PAI**, is obtained by consecutive C–N/C–C bond formation between diphenylamines and 9,10-dibromoperylenecarboximide. Owing to the rigid structure, extended π-conjugation and pronounced push-pull substitution, these fluorophores show emission maxima up to 804 nm and large Stokes shifts. The extraordinarily high fluorescence quantum yields from 47 % to 70 % are attributed to chloro substitution in the bay positions of the perylene core. These characteristics, together with high photostability, qualify them as useful NIR emitters for applications as biomarkers and security inks.

Near-infrared (NIR) fluorophores which can release radiation at wavelengths beyond 700 nm upon excitation are of great value for many cutting-edge applications, from bioimaging[1] and photodynamic therapy[2] to photoelectronics[3] and security printing.[4] When compared to inorganic counterparts, organic fluorophores show advantages in view of structural versatility, long-term biosafety and biocompatibility.[5] Organic NIR fluorophores include conjugated polymers and metal complexes,[6] but mainly small molecules such as cyanines,[7] squaraines,[8] BODIPYs,[9] phthalocyanines[10] and porphyrins.[11] Most organic NIR colorants, however, suffer from low fluorescence quantum yields (Φ_{fl}) due to an increased contribution of non-radiative decay as suggested by the energy gap law for S_1–S_0 internal conversion (IC).[12] Despite enormous efforts over recent years, organic colorants with emission maxima (λ_{em}) beyond 800 nm rarely have Φ_{fl} above 20 % (Table S3).[13] It still remains a challenge to develop bright deep-NIR fluorophores, let alone photostability[5] and large Stokes shift[14] which are highly required for practical applications.

The following design principles (Figure 1) have been employed in our access to NIR emitters. Chromophore **3**, made from perylenecarboximide **1**, has remarkable photostability and far-red fluorescence at $\lambda_{em} = 666$ nm with Φ_{fl} of

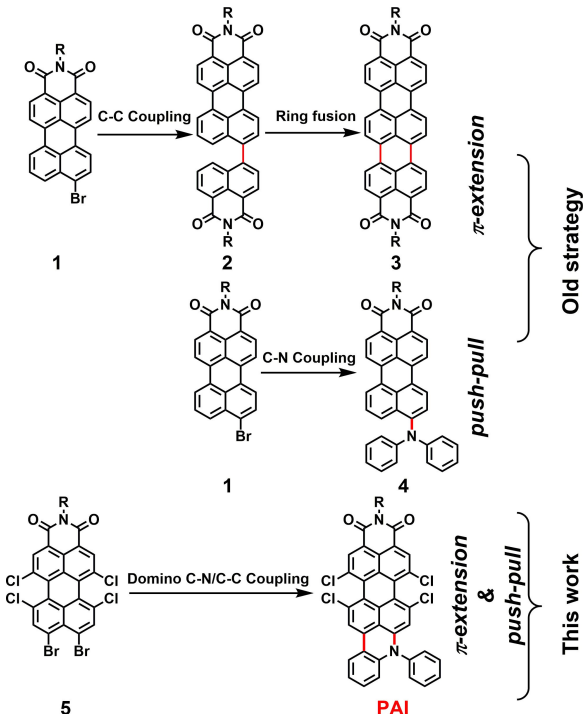

Figure 1. Synthetic strategy toward NIR fluorophores.

[*] Dr. Z.-H. Wu, Dr. A. Skabeev, Prof. Dr. K. Müllen, Dr. C. Li
Max-Planck Institute for Polymer Research
Ackermannweg 10, 55128 Mainz (Germany)
E-mail: muellen@mpip-mainz.de
lichen@dgut.edu.cn
Dr. R. Duan, Dr. C. Li
School of Materials Science and Engineering, Dongguan University of Technology
No. 1 Daxue Rd., Songshan Lake, Dongguan City, 523820
Guangdong Province (P. R. China)
Prof. Dr. Y. Zagranyarski
Fac Chem & Pharm, Sofia Univ. St Kliment Ohridski
1 James Bourchier Blvd, Sofia 1164 (Bulgaria)
Prof. Dr. J.-O Jin
Department of Microbiology, University of Ulsan College of Medicine
ASAN Medical Center, Seoul 05505 (South Korea)
Prof. Dr. M. Kwak
Department of Chemistry, Pukyong National University
Busan 48513 (South Korea)
Dr. Z.-H. Wu, Prof. Dr. T. Basché, Prof. Dr. K. Müllen
Department of Chemistry, Johannes Gutenberg-University
55099 Mainz (Germany)
E-mail: basche@uni-mainz.de

70 %, but narrow Stokes shift (13 nm).[15] On the other hand, the push-pull substituted derivative **4** exhibits a Stokes shift larger than 80 nm, but absorption and emission short of the NIR region.[16] Combining both concepts, i.e., π-extension for a bathochromic shift and donor-acceptor substitution toward enhanced Stokes shift,[17] NIR fluorescent **PAI**s, fusion of diphenylamines and perylenecarboximide, are obtained through an efficient consecutive C–N/C–C bond formation. Remarkably, it turned out that the extremely high Φ_{fl}-values are related to the chloro substitution in the bay positions of the perylene core which leads to a decrease of the IC rate in comparison to the dechlorinated analogues, **PAI′**. Compound **PAI-e** substituted by bis(4-diphenylaminophenyl)amine exhibits λ_{em} at 804 nm with a high Φ_{fl} of 59 %. **WS-PAI-e**, a modification containing sulfonic acid groups, demonstrated promising performance in preliminary cellular uptake.

As shown in Scheme 1, compound **6** was synthesized by chlorination of perylenetetracarboxylic dianhydride followed by the Hunsdiecker reaction.[18] The Buchwald–Hartwig C–N coupling of **6** with diphenylamine mediated by palladium (II) acetate [$Pd(OAc)_2$] as catalyst and tricyclohexylphosphine (PCy_3) as ligand failed to furnish the doubly aminated product **7**, but rather gave **9** as main product with a new C–C bond formed between **6** and the α-phenyl position of the diphenylamine. Mass spectrometry indicated debrominated compound **10** as a byproduct in only trace amounts. The formation of **9** includes two steps, firstly, the amination and secondly, the C–C coupling under C–H-activation (details see ESI).[19]

Considering the two-step mechanism, various catalyst systems for amination and activated C–H coupling were tested. The results pointed toward a catalyst/ligand combination of tris(dibenzylideneacetone)dipalladium(0) [$Pd_2(dba)_3$]/tri-tert-butylphosphine (*t*-Bu_3P) and $Pd(OAc)_2/PCy_3$ in toluene at 100 °C giving the most favorable ratio of **9a/b** and **10**. Single crystals of **9a** were obtained by slow diffusion of hexane into a CH_2Cl_2 solution.[20] According to single-crystal X-ray diffraction (Figure 2), the tetrachloro substituted perylene core of **9a** adopts a highly twisted structure with a dihedral angle between the two naphthalene planes of 31°. The molecules pack in a head-to-tail manner with the electron-donating diphenylamino moieties placed on top of the neighboring anhydride units. The apparent lamellar motif can be ascribed to the asymmetrical structure and oriented charge distribution. It is markedly different from that present in most perylene dyes, which are commonly packed in a herringbone fashion.[21]

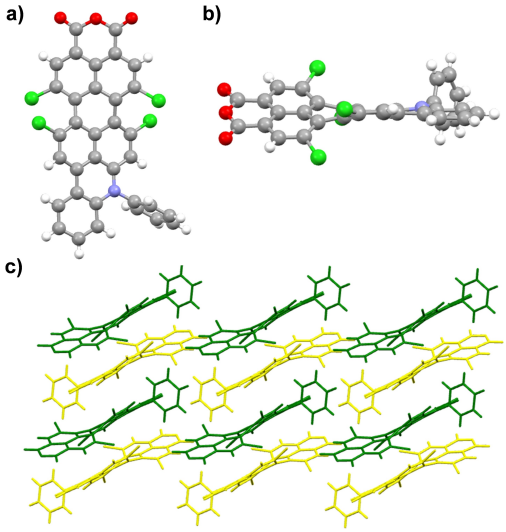

Figure 2. Crystal structure of **9a** in a) top, and b) side views. c) Packing diagram viewed from b axis.

However, using the anhydride **6** as the starting material had practical disadvantages such as strong aggregation in solution and a tendency to stick on silica, limiting the yield of **9a/b** to 35–45 %. The additional step of imidization of **6** (Scheme 2) to afford carboximide **5** allowed us to circumvent these problems.[18] Compound **5** exhibited much better solubility than **6** and could be easily purified via either recrystallization or column chromatography. Using **5** and different diphenylamines as reactants, a series of NIR

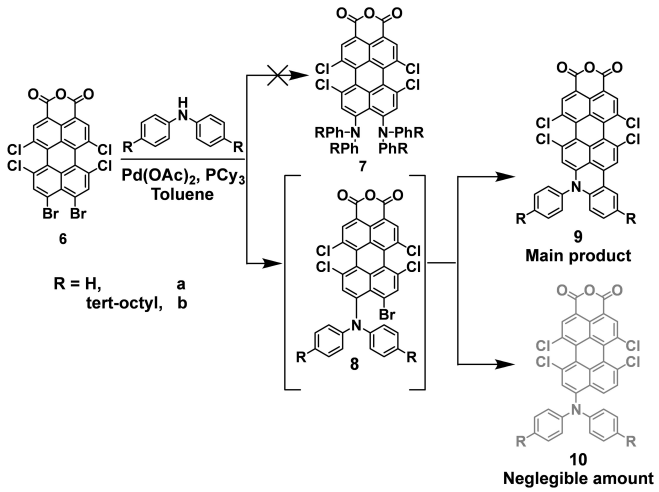

Scheme 1. Synthesis toward **9**.

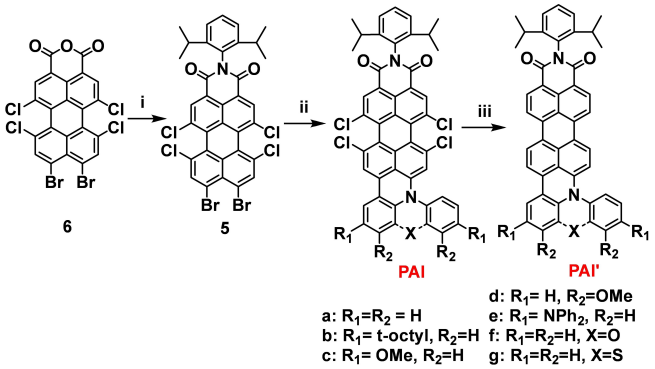

Scheme 2. Synthesis toward **PAI** and **PAI′**. Reagents and conditions: (i) 2,6-Diisopropylaniline, NMP, AcOH, 110 °C, overnight, 79 %; (ii) Diphenylamines, $Pd(OAc)_2$, $Pd_2(dba)_3$, t-Bu_3P, Cy_3P, toluene, 100 °C, 1–12 h, 40–70 %; (iii) KOH, ethylene glycol, 165 °C, 20–24 h, 52–91 %.

fluorophores **PAI**s were synthesized under the optimized C–N/C–C domino reaction condition in yields of 40–70 %. In addition, **5** can react with phenoxazine (**PAI-f**) and phenothiazine (**PAI-g**), while 4,5-dibromo-naphthalene-1,8-dicarboximide and diphenylamines can provide **12** (see ESI). Finally, dehalogenation of **PAI** by refluxing with potassium hydroxide in ethylene glycol produced the dechlorinated chromophores **PAI′** in yields of 52 %–91 %. All compounds were fully characterized by NMR spectroscopy, mass spectrometry and elemental analysis.

All **PAI** chromophores (Table S1 and Figure S2) exhibit strong absorptions (molar extinction coefficients ε in the range of 4–6×10^4 $M^{-1}cm^{-1}$) located between 550 and 800 nm, achieving prominent bathochromic shifts more than 100 nm when compared to the reported perylenecarboximides **4** with only a donor function.[16] Most noteworthy is the high NIR Φ_{fl} of **PAI**s, featuring values from 47 % to 70 % within the 700–1000 nm range. To address the origin of the large Φ_{fl}, we have dechlorinated the **PAI**s to obtain **PAI′**s. As a general trend, the **PAI′**s are characterized by considerably smaller Φ_{fl} which we exemplarily discuss for the case **PAI-b** vs. **PAI′-b**. Besides the Φ_{fl} of both compounds, we also measured their fluorescence lifetime (τ_{fl}). As shown in Table 1, both Φ_{fl} and τ_{fl} decrease in harmony by a factor of ≈2.1 after dechlorination. Using $k_{rad}=\Phi_{fl}\ (\tau_{fl})^{-1}$, we found the radiative rates (k_{rad}) of both compounds to be almost equal, which is very reasonable taking into account the similar emission wavelengths. The non-radiative rate (k_{nr}) obtained by $k_{nr}=(\tau_{fl})^{-1}-k_{rad}$, however, is roughly a factor of 5 smaller for **PAI-b** compared to **PAI′-b**. From the literature, it is well known that perylenecarboximides have very small intersystem crossing (ISC) rates.[22] Moreover, if ISC would play a role at all, chlorination and the concomitant twisting of the perylene core should lead to an increase of the ISC rate.[23] In contrast, we observed a decrease of the non-radiative rate after chlorination. Accordingly, we rule out ISC as a relevant contribution and identify the non-radiative relaxation with IC. It is commonly believed that high frequency C–H-stretching vibrations serve as accepting modes in S_1–S_0 IC process.[24] Replacing the hydrogen atoms in the bay region of the perylene core in **PAI′-b** by chlorine atoms (**PAI-b)** will lead to a strong decrease of the corresponding vibrational stretching frequencies. Assuming that the C–Cl-vibrations still serve as accepting modes of the electronic excitation energy, a larger number of vibrational quanta is needed for energy take-up, rendering non-radiative relaxation less probable.[25] Along these lines, the substantial decrease of the Φ_{fl} upon dechlorination supports the notion that the C–H stretching vibrations of hydrogen atoms in the bay region of the perylene core strongly promote non-radiative decay. Considering perylene- and terrylenecarboximides which emit at shorter wavelengths, similar effects of chlorination may have gone unnoticed, as radiative decay is the primary relaxation channel in these compounds.[25] In addition to a change of the vibrational frequencies, the chloro-substitution may also impact to a minor extent the fluorescence properties via the electron-withdrawing properties of the C–Cl bonds as well as the Cl-induced twisting of the perylene core.

PAI-e, with the strongest electron-donating substitution as well as absorption and emission maxima at 723 and 804 nm, respectively, was used for further experiments to study its prospects in cellular uptake and as security ink. In this case, Φ_{fl} of 55 % was achieved in dichloromethane against a reference dye (Rhodamine 800), which compares nicely to an absolute measurement in an integrating sphere which yielded 59 % (Figure S3). Toward preliminary cell uptake experiments, **PAI-e** was decorated with tetraethylenglycol and sulfonic acid groups to produce **TEG-PAI-e** and **WS-PAI-e**, respectively (ESI). The cellular uptake analysis in HeLa cells was carried out by flow cytometry (Figure 3b and S7). In comparison with **TEG-PAI-e**, **WS-PAI-e** demonstrated superior uptake performance, mainly attributed to its higher water solubility. As illustrated in Figure 3b, the cells incubated with 1μg/mL **WS-PAI-e** displayed a significant NIR fluorescence signal in contrast to the cells incubated without **WS-PAI-e**, indicating the successful cellular uptake of **WS-PAI-e**. Moreover, the fluorescence signal intensity of **WS-PAI-e** exhibited a dose-dependent increase, confirming its efficient uptake. The cell uptake of **WS-PAI-e** was further visualized by co-staining experiments with confocal laser scanning microscopy. As shown in Figure 3c, on the basis of the blue emission of 4′,6-diamidino-2-phenylindole (DAPI, λ_{em} at 461 nm), the NIR emission of **WS-PAI-e** could be observed clearly with a high signal to noise ratio. The cytotoxic activity of **WS-PAI-e** for HeLa cells was evaluated by MTT (3-(4,5-dimethylthiazol-2-yl)-2,5-diphenyltetrazolium bromide) assays (Figure S6c). After incubation with **WS-PAI-e** at concentrations from 0.1 to 5 μg/mL for 24 hours, the cell viabilities were close to 100 %, underlining low cytotoxicity of **WS-PAI-e**. Additionally, the fluorescence intensity remained almost identical under 24 hours continuous monitoring (Figure S6), indicating **WS-PAI-e** as much more stable than most commercial NIR fluorescent dyes such as Cy7 and Cy7.5. These results from preliminary cell uptake and staining experiments illustrated the potential of **WS-PAI-e** as an effective NIR fluorescence agent.

Table 1: Spectroscopic and photophysical data of **PAI-b** and **PAI′-b**.

	λ_{ab} nm	λ_{em} nm	$\Phi_{fl}^{(a)}$ %	τ_{fl} ns	k_{rad} 10^8 s^{-1}	k_{nr} 10^8 s^{-1}
PAI-b	675	726	65	4.7	1.4	0.7
PAI′-b	705	730	31	2.1	1.5	3.3

[a] Measured in toluene against Rhodamine 800 in ethanol as a reference ($\Phi_{fl}=0.25$).[26]

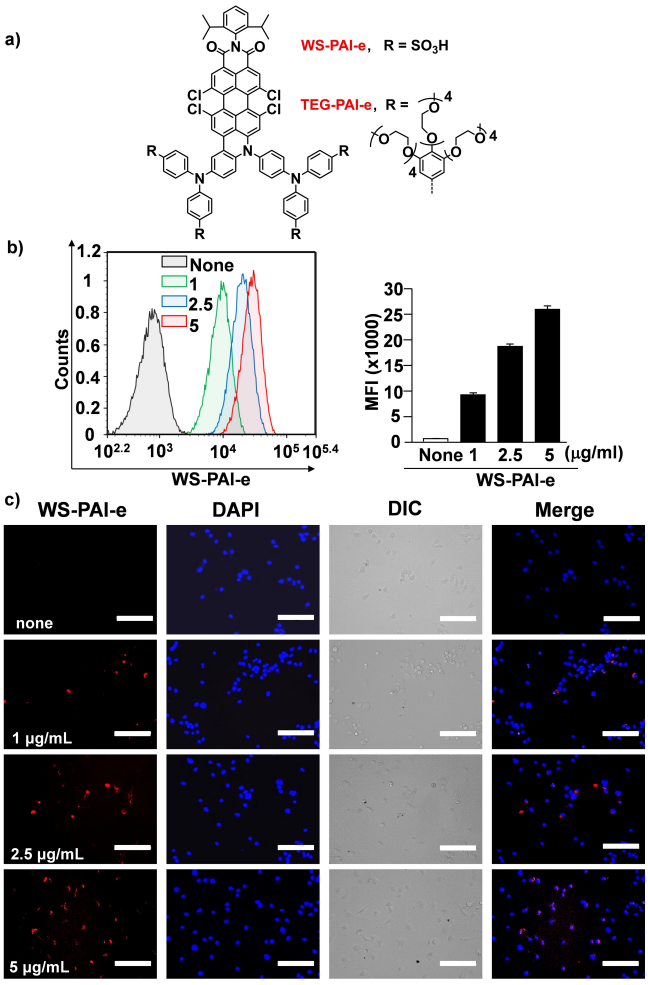

Figure 3. a) Molecular structures of **TEG-PAI-e** and **WS-PAI-e**. b) Flow cytometry analysis of cellular uptake of **WS-PAI-e** in a concentration dependent manner (after 24 h uptake). MFI: mean fluorescence intensity. c) Confocal fluorescence images of **WS-PAI-e** in HeLa cells at different concentrations; WS-PAI-e: **WS-PAI-e** treated cells; DAPI: cell nucleus stained with DAPI; DIC: differential interference microscopy image of cells, i.e. bright field; Merge: double-color staining images. Scale bars: 150 μm.

The absorption and emission domains of **PAI-e** are 600–800 nm and 700–1000 nm, respectively, enabling excitation and emission both in the NIR region. These characteristics are desirable in applications such as security printing, where the interference with visible light (400–700 nm) should be avoided. Considering the negligible visible absorption, good photostability and high NIR Φ_{fl}, a security ink was prepared by mixing polymethylmethacrylate (PMMA) with **PAI-e** in dichloromethane (10^{-5} M).[27] The colorless ink (Figure 4d) was directly drop-cast onto a glass coverslip with grid width and depth of 5 μm each (Ibidi, Grid-50). By imaging with a fluorescence microscope (Thunder Imager from Leica), the coating was not visible under white light (Figure 4a), but visible after excitation by NIR light at 730 nm under fluorescence imaging conditions (Figure 4b). It follows that **PAI-e**-based inks can be coated on colored as well as non-colored surfaces with the resulting coatings only being

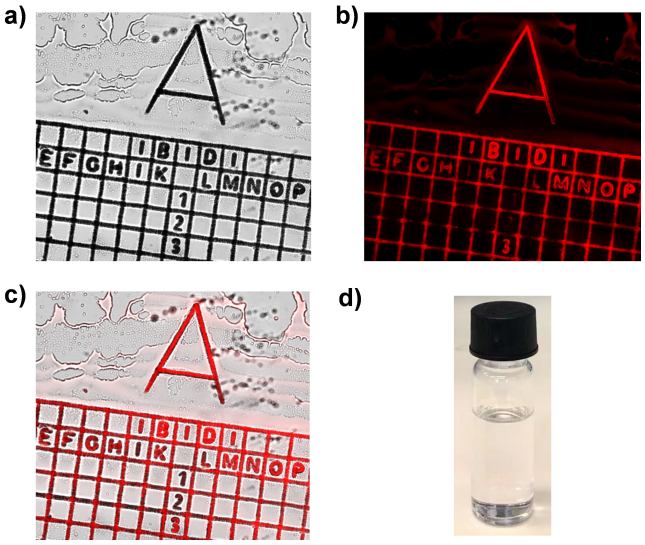

Figure 4. Invisible ink based on **PAI-e**: a) Image under white light. b) Fluorescence image (compatible emission bandpass from 770–850 nm) under excitation light at 730 nm. c) Overlay of the fluorescence and white light images. d) The mixed solution of compound **PAI-e** and PMMA (0.08 mg/mL) in dichloromethane.

detectable under NIR light excitation and with a NIR camera.

In conclusion, we have developed a novel series of perylenecarboximide-based fluorescent dyes which can be obtained readily via C–N/C–C domino reactions. Owing to the extended π-conjugation and pronounced push-pull substitution, these fluorophores show NIR emission in the range from 700 to 1000 nm with high fluorescence quantum yield and large Stokes shift. Exemplarily, **PAI-e**, with the highest absorption and emission maxima, exhibits a Stokes shift of 81 nm and fluorescence quantum yield of 59 %, which qualifies **PAI-e** as an applicable fluorophore for use in low concentration. Low doses make the **PAI-e** not only colorless, but also non-toxic. Thus, **PAI-e** makes the spectral region between 750 and 850 nm accessible for various applications such as bio-imaging and security inks.

Acknowledgements

We acknowledge the Microscopy Core Facility at the Institute of Molecular Biology (IMB Mainz) for the use of the microscopes and technical support. Open Access funding enabled and organized by Projekt DEAL.

Conflict of Interest

The authors declare no conflict of interest.

Data Availability Statement

The data that support the findings of this study are available from the corresponding author upon reasonable request.

Keywords: Biomarkers · Consecutive C–N/C–C Coupling Reactions · Fluorescence Quantum Yields · Near-Infrared · Rylenecarboximide

[1] a) J. Li, Y. Dong, R. Wei, G. Jiang, C. Yao, M. Lv, Y. Wu, S. H. Gardner, F. Zhang, M. Y. Lucero, J. Huang, H. Chen, G. Ge, J. Chan, J. Chen, H. Sun, X. Luo, X. Qian, Y. Yang, *J. Am. Chem. Soc.* **2022**, *144*, 14351; b) S. Zhang, W. Yang, X. Lu, X. Zhang, Z. Pan, D.-H. Qu, D. Mei, J. Mei, H. Tian, *Chem. Sci.* **2023**, *14*, 7076.

[2] X. Li, J. F. Lovell, J. Yoon, X. Chen, *Nat. Rev. Clin. Oncol.* **2020**, *17*, 657.

[3] a) T. Huang, H. Chen, J. Feng, A. Zhang, W. Jiang, F. He, Z. Wang, *ACS Materials Lett.* **2019**, *1*, 404; b) M. Casutt, M. Ruscello, N. Strobel, S. Koser, U. H. F. Bunz, D. Jänsch, J. Freudenberg, G. Hernandez-Sosa, K. Müllen, *Chem. Mater.* **2019**, *31*, 7657.

[4] H. Liu, J. Xu, H. Wang, Y. Liu, Q. Ruan, Y. Wu, X. Liu, J. K. W. Yang, *Adv. Mater.* **2019**, *31*, 1807900.

[5] a) Y. Liu, Y. Li, S. Koo, Y. Sun, Y. Liu, X. Liu, Y. Pan, Z. Zhang, M. Du, S. Lu, X. Qiao, J. Gao, X. Wang, Z. Deng, X. Meng, Y. Xiao, J. S. Kim, X. Hong, *Chem. Rev.* **2022**, *122*, 209; b) D. C. Young, M. Tasior, A. D. Laurent, Ł. Dobrzycki, M. K. Cyrański, N. Tkachenko, D. Jacquemin, D. T. Gryko, *J. Mater. Chem. C* **2020**, *8*, 7708; c) T. Shen, D. Dijkstra, A. Farrando-Pérez, P. G. Boj, J. M. Villalvilla, J. A. Quintana, Ya. Zou, X. D. Hou, H. P. Wei, Z. T. Li, Z. Sun, M. A. Díaz-García, J. Wu, *Angew. Chem. Int. Ed.* **2023**, *62*, e202304197.

[6] a) W. Li, B. Wang, T. Miao, J. Liu, G. Fu, X. Lü, W. Feng, W.-Y. Wong, *J. Mater. Chem. C* **2021**, *9*, 173; b) T. N. Nguyen, S. V. Eliseeva, A. Gładysiak, S. Petoud, K. C. Stylianou, *J. Mater. Chem. A* **2020**, *8*, 10188.

[7] H. Ma, Y. Lu, Z. Huang, S. Long, J. Cao, Z. Zhang, X. Zhou, C. Shi, W. Sun, J. Du, J. Fan, X. Peng, *J. Am. Chem. Soc.* **2022**, *144*, 3477.

[8] M. H. Chua, H. Zhou, T. T. Lin, J. Wu, J. Xu, *ACS Omega* **2018**, *3*, 16424.

[9] R. Tiwari, P. S. Shinde, S. Sreedharan, A. K. Dey, K. A. Vallis, S. B. Mhaske, S. K. Pramanik, A. Das, *Chem. Sci.* **2021**, *12*, 2667.

[10] S. Abid, S. Ben Hassine, N. Richy, F. Camerel, B. Jamoussi, M. Blanchard-Desce, O. Mongin, F. Paul, C. O. Paul-Roth, *Molecules* **2020**, *25*, 239.

[11] a) R. Weinstain, T. Slanina, D. Kand, P. Klan, *Chem. Rev.* **2020**, *120*, 13135; b) R. W. Hooper, A. Zhang, D. Koszelewski, J. P. Lewtak, B. Koszarna, C. J. Levy, D. T. Gryko, M. J. Stillman, *J. Porphyrins Phthalocyanines* **2018**, *22*, 1111.

[12] a) R. Englman, J. Jortner, *Mol. Phys.* **1970**, *18*, 145; b) C. Erker, T. Basché, *J. Am. Chem. Soc.* **2022**, *144*, 14053.

[13] a) H. U. Kim, T. Kim, C. Kim, M. Kim, T. Park, *Adv. Funct. Mater.* **2023**, *33*, 2208082; b) L. Zhang, C. Liu, S. Zhou, R. Wang, Q. Fan, D. Liu, W. Wu, X. Jiang, *Nat. Photonics* **2022**, *16*, 843.

[14] C. S. Abeywickrama, H. J. Baumann, N. Alexander, L. P. Shriver, M. Konopka, Y. Pang, *Org. Biomol. Chem.* **2018**, *16*, 3382.

[15] a) K. S. Mehra, S. Jha, A. M. Menon, D. Chopra, J. Sankar, *Chem. Sci.* **2023**, *14*, 3147; b) F. Holtrup, G. Müller, H. Quante, S. de Feyter, F. C. De Schryver, K. Müllen, *Chem. Eur. J.* **1997**, *3*, 219.

[16] X. Zhang, A. Elmali, R. Duan, Q. Liu, W. Ji, J. Zhao, C. Li, A. Karatay, *Phys. Chem. Chem. Phys.* **2020**, *22*, 6376.

[17] A. Borissov, Y. K. Maurya, L. Moshniaha, W.-S. Wong, M. Żyła-Karwowska, M. Stępień, *Chem. Rev.* **2022**, *122*, 565.

[18] Y. Zagranyarski, L. Chen, Y. F. Zhao, H. Wonneberger, C. Li, K. Müllen, *Org. Lett.* **2012**, *14*, 5444.

[19] a) M. Mahl, K. Shoyama, J. Rühe, V. Grande, F. Würthner, *Chem. Eur. J.* **2018**, *24*, 9409; b) Y. Zagranyarski, A. Skabeev, Y. Ma, K. Müllen, C. Li, *Org. Chem. Front.* **2016**, *3*, 1520.

[20] Deposition number 2092586 (**9a**) contains the supplementary crystallographic data for this paper. These data are provided free of charge by the joint Cambridge Crystallographic Data Centre and Fachinformationszentrum Karlsruhe Access Structures service.

[21] C. Ramanan, A. Smeigh, J. Anthony, T. Marks, M. Wasielewski, *J. Am. Chem. Soc.* **2012**, *134*, 386.

[22] E. Lang, R. Hildner, H. Engelke, P. Osswald, F. Würthner, J. Köhler, *ChemPhysChem* **2007**, *8*, 1487.

[23] a) K. Nagarajan, A. R. Mallia, K. Muraleedharan, M. Hariharan, *Chem. Sci.* **2017**, *8*, 1776; b) Y. Wu, Y. Zhen, Y. Ma, R. Zheng, Z. Wang, H. Fu, *J. Phys. Chem. Lett.* **2010**, *1*, 2499.

[24] N. J. Turro, V. Ramamurthy, J. C. Scaiano, *Modern Moleular Photochemistry of Organic Molecules*, University Science Books **2010**.

[25] a) A. Nowak-Król, K. Shoyama, M. Stolte, F. Würthner, *Chem. Commun.* **2018**, *54*, 13763; b) K. Rani, U. K. Pandey, S. Sengupta, *J. Mater. Chem. C* **2021**, *9*, 4607.

[26] A. Alessi, M. Salvalaggio, G. Ruzzon, *J. Lumin.* **2013**, *134*, 385.

[27] Z. Lei, X. Li, X. Luo, H. He, J. Zheng, X. Qian, Y. Yang, *Angew. Chem. Int. Ed.* **2017**, *56*, 2979.

Manuscript received: October 9, 2023
Accepted manuscript online: November 10, 2023
Version of record online: November 23, 2023